

RESEARCH ARTICLE

Diffusion-Weighted Imaging for the Left Hepatic Lobe has Higher Diagnostic Accuracy for Malignant Focal Liver Lesions

Xue Han, Yin Dong, Jian-Jun Xiu, Jie Zhang, Zhao-Qin Huang, Shi-Feng Cai, Xian-Shun Yuan, Qing-Wei Liu*

Abstract

Background: This study was conducted to investigate whether apparent diffusion coefficient (ADC) measurements by dividing the liver into left and right hepatic lobes may be utilized to improve the accuracy of differential diagnosis of benign and malignant focal liver lesions. **Materials and Methods:** A total of 269 consecutive patients with 429 focal liver lesions were examined by 3-T magnetic resonance imaging that included diffusion-weighted imaging. For 58 patients with focal liver lesions of the same etiology in left and right hepatic lobes, ADCs of normal liver parenchyma and focal liver lesions were calculated and compared using the paired t-test. For all 269 patients, ADC cutoffs for focal liver lesions and diagnostic accuracy in the left hepatic lobe, right hepatic lobe and whole liver were evaluated by receiver operating characteristic curve analysis. **Results:** For the group of 58 patients, mean ADCs of normal liver parenchyma and focal liver lesions in the left hepatic lobe were significantly higher than those in the right hepatic lobe. For differentiating malignant lesions from benign lesions in all patients, the sensitivity and specificity were 92.6% and 92.0% in the left hepatic lobe, 94.4% and 94.4% in the right hepatic lobe, and 90.4% and 94.7% in the whole liver, respectively. The area under the curve of the right hepatic lobe, but not the left hepatic lobe, was higher than that of the whole liver. **Conclusions:** ADCs of normal liver parenchyma and focal liver lesions in the left hepatic lobe were significantly higher than those in the right hepatic lobe. Optimal ADC cutoff for focal liver lesions in the right hepatic lobe, but not in the left hepatic lobe, had higher diagnostic accuracy compared with that in the whole liver.

Keywords: Diffusion-weighted imaging - apparent diffusion coefficient - focal liver lesion - left and right hepatic lobes

Asian Pac J Cancer Prev, 15 (15), 6155-6160

Introduction

Diffusion weighted imaging (DWI) is increasingly used for the detection, characterization and diagnosis of various diseases (Naiki et al., 2011; Wu et al., 2013), especially focal liver lesions (Taouli, 2012). Apparent diffusion coefficient (ADC) provides quantitative characterization of liver lesions and helps discrimination between benign and malignant focal liver lesions.

Despite widespread clinical use of such an advanced magnetic resonance imaging (MRI) technique, DWI in the abdomen is still known to be highly sensitive to organ motions (Naganawa et al., 2005; Dietrich et al., 2010; Taouli and Koh, 2010). Several studies reported that cardiac motion has an impact on DWI of abdomen, resulting in higher ADC of normal liver parenchyma in left compared with right hepatic lobes (Mürtz et al., 2002; Nasu et al., 2006; Kiliçkesmez et al., 2008; Kandpal et al., 2009; Kwee et al., 2009; Schmid-Tannwald et al., 2013). In addition, Schmid-Tannwald et al. (2013) reported that ADC of benign and malignant focal liver lesions calculated from noncardiac-gated DWI were significantly

higher in the left hepatic lobe. Therefore, variations of ADC of focal liver lesions caused by their locations in the liver may indicate an important limitation of DWI, and potentially impact effectiveness for characterizing focal liver lesions. However, by dividing the liver into left and right hepatic lobes instead of regarding it as a whole, the ADC cutoffs for focal liver lesions may be different. In addition, the diagnostic accuracy for lesion discrimination using different ADC cutoffs in left hepatic lobe, right hepatic lobe and whole liver may also be different. However, such studies are limited.

The first purpose of the present study was to measure and compare ADCs of normal liver parenchyma and focal liver lesions in left hepatic lobe and right hepatic lobe, and to determine whether ADCs of normal liver parenchyma and focal liver lesions, calculated from noncardiac-gated DWI acquisitions, are different in left hepatic lobe and right hepatic lobe. The second purpose of this study is to characterize focal liver lesions in each hepatic lobe, and to differentiate malignant lesions from benign lesions using different ADC cutoffs in left hepatic lobe, right hepatic lobe and whole liver.

Materials and Methods

Patients

Through a retrospective search in the radiology patient database, 356 consecutive patients with focal liver lesions (excluding hepatic cysts) underwent abdominal magnetic resonance examination of the liver between October 2010 and March 2013. Eighty-seven patients were excluded from our analysis under exclusion criteria: i) focal liver lesions with the diameter < 1 cm were present (in order to avoid gross errors due to partial volume effects), ii) sufficient confirmation of the nature of the lesions was not available, iii) distinct artifacts were observed on DWI, and iv) chemotherapy and radiofrequency ablation had been performed within the last 12 months prior to the magnetic resonance examination (in order to ensure that ADC measurements were reflective of the natural state of liver lesions). Hence, our retrospective analysis included 269 patients (180 males, 89 females, age range of 21-80 years and mean age 54.7 years). Multiple lesions were present in 94 of the 269 patients. In patients with the number of lesions ≥ 5 for each lesion type, five lesions were randomly selected for quantitative measurements by the study coordinator. Thus, a total of 429 hepatic lesions were included. The type and distribution of focal liver lesions are shown in Table 1.

Three hundred and four patients had malignant tumors, including 23 with cholangiocellular carcinomas (CCC), 120 with hepatocellular carcinomas (HCC) and 161 with metastases. For all patients with CCC, 58 patients with HCC and 33 patients with metastases, histopathologic verification of the lesions by means of biopsy and/or surgery was available. The diagnosis of the remaining HCC and metastases was established on the basis of typical MRI findings, clinical history, pathologic tracer uptake of the lesions by positron emission tomography-computed tomography, and follow-up imaging studies. There were a total of 125 cases of benign lesions, including 9 cases of focal nodular hyperplasias and 116 cases of hemangiomas. Histopathologic verification was available in 5 cases of focal nodular hyperplasias and 5 cases of hemangiomas. The remaining cases of benign lesions showed typical MRI findings (Horton et al., 1999; Bartolozzi et al., 2001; Bruegel et al., 2008) in conjunction with stability in lesion size and morphology on serial cross-sectional imaging studies with a minimal follow-up interval of 6 months.

For the investigation in which the liver was divided into left and right hepatic lobes, we studied 58 patients (37 males and 21 females, with a mean age of 54.4 years) who were selected from all 269 patients, including 2 with 4 CCC, 16 with 32 HCC, 17 with 34 metastases and 23 with 46 hemangiomas. The inclusion criteria were: i) the patient at least had two focal liver lesions, one in left hepatic lobe and the other in right hepatic lobe; ii) the two lesions in left hepatic lobe and right hepatic lobe, respectively, in each patient were of the same etiology and similar MRI features; and iii) the two lesions in each patient had similar sizes. Patients whose focal liver lesions possessed large regions of necrosis and cystic degeneration were excluded. For other studies, all 269 patients were investigated.

This study was approved by the Ethics Committee

Table 1. Types and Distribution of Focal Liver Lesions

| | Malignant | | | Benign | | Total |
|-------|-----------|-----|------------|------------|-----|-------|
| | CCC | HCC | Metastases | Hemangioma | FNH | |
| LHL | 13 | 34 | 78 | 50 | 4 | 179 |
| RHL | 10 | 86 | 83 | 66 | 5 | 250 |
| Total | 23 | 120 | 161 | 116 | 9 | 429 |

*Note: CCC, cholangiocellular carcinoma; HCC, hepatocellular carcinoma; FNH, focal nodular hyperplasia; LHL, left hepatic lobe; RHL, right hepatic lobe.

Table 2. ADCs of NLP and FLLs (benign and malignant) in LHL and RHL (means \pm standard deviation; $\times 10^{-3}$ mm²/sec) in the 58 Patients with Focal Liver Lesions of the Same Etiology in Left and Right Hepatic Lobes.

| | LHL | RHL | P value |
|----------------|-----------------|-----------------|---------|
| NLP | 1.69 \pm 0.21 | 1.35 \pm 0.17 | <0.001 |
| Benign FLLs | 2.38 \pm 0.62 | 1.88 \pm 0.57 | <0.001 |
| Malignant FLLs | 1.21 \pm 0.25 | 0.98 \pm 0.20 | <0.001 |

*Note: NLP, normal liver parenchyma; FLL, focal liver lesions; LHL, left hepatic lobe; RHL, right hepatic lobe. Paired t-test was used for statistical analysis.

of Provincial Hospital of Shandong University. Written informed consent was obtained from all patients or their families.

MRI

All patients were examined on a 3.0-T MRI system (Magnetom Verio, Siemens, Germany). Patients were imaged in the supine with a surface phased-array coil. For full evaluation of the focal liver lesions, breath-hold transverse T2-weighted fast spin-echo sequences (repetition time [TR], 3000-4000 ms; echo time [TE], 90-104 ms) were initially performed, followed by transverse T1-weighted dual-echo in-phase and out-of-phase sequences (flip angle, 70 degrees; TR, 130; TE, 2.3 ms in phase; TE, 3.7 ms out of phase) with a 5-mm slice thickness and 1-mm interspace. Three-dimensional fat-saturated T1-weighted dynamic contrast-enhanced sequence (volume interpolated body examination, Siemens, Germany) was given during suspended respiration. Gadobenate dimeglumine (Gd-BOPTA, MultiHance; 0.1 mmol/kg) was injected intravenously at a rate of 2.5 ml/s by a power injector, followed by a 20-mL saline flush. Dynamic contrast-enhanced MRI was performed in the transverse plane with a 3-mm slice thickness and no interspace at baseline (precontrast), the hepatic arterial-dominant phase (20-25 seconds), portal venous (60-70 seconds), equilibrium phase (180-200 seconds), and hepatocellular phase (90 minutes) after contrast injection, respectively.

Before dynamic contrast-enhanced imaging, transverse respiratory triggered DW single-shot echo-planar imaging (SS-EPI) sequence was performed with tri-directional diffusion gradients by using two b values of 0 and 800 sec/mm². For shortening acquisition time, integrated parallel imaging techniques (iPAT) by means of generalized autocalibrating partially parallel acquisitions (Griswold et al., 2002; Bruegel et al., 2008) with a 2-fold acceleration factor were used. For respiratory triggering, prospective acquisition correction was implemented. The prospective acquisition correction technique interleaves the imaging sequence with a navigator sequence. The information

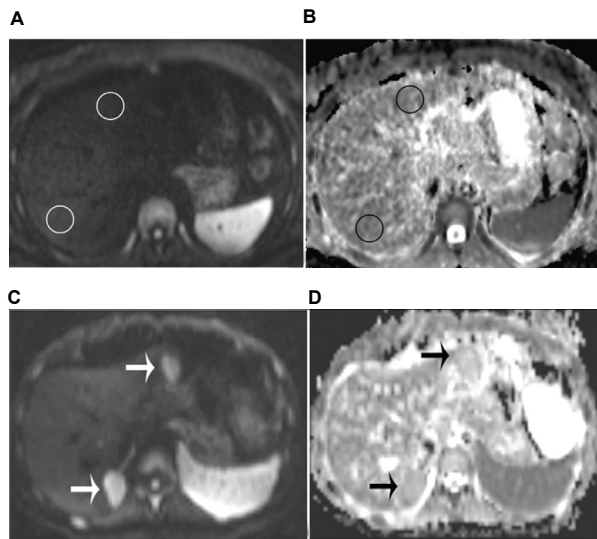


Figure 1. ADC Measurement of Normal Liver Parenchyma in a 43-year-old Female with Focal Nodular Hyperplasia and Hemangiomas from A 36-year-old Female. (A) Diffusion-weighted image ($b = 800 \text{ sec/mm}^2$) of a 43-year-old female. (B) ADC map of a 43-year-old female. The region of interest of normal liver parenchyma was drawn without involving intrahepatic vessels. ADCs in left hepatic lobe and right hepatic lobe were $1.58 \times 10^{-3} \text{ mm}^2/\text{sec}$ and $1.36 \times 10^{-3} \text{ mm}^2/\text{sec}$, respectively. (C) Diffusion-weighted image ($b = 800 \text{ sec/mm}^2$) of a 36-year-old female showing hyperintensity of both hemangiomas (arrows). (D) ADC map of a 36-year-old female.

gained with the navigator is used to synchronize the measurement with the patient's breathing cycle and to place the data acquisition period into the end-expiration phase. The number of sections acquired per respiratory cycle (i.e., the number of sections per block) is adjusted to fit the individual breathing cycle of the patients. ADC maps were generated with a commercially available software workstation system (Syngo Multimodality workplace, Siemens, Germany). The technical parameters were as follows: TR, 4000 ms; TE, 73 ms; echo train length, 92; receiver bandwidth, 2442 Hz/pixel; number of signal averages, 3; section thickness, 5 mm; intersection gap, 1 mm; 30-35 transverse sections acquired; acquisition time, 4-6 min.

Image analysis

Review of all magnetic resonance images and follow-up imaging studies (MRI, CT, or/and PET-CT) was performed on a PACS workstation (GE Healthcare, USA). The magnetic resonance images were analyzed by two radiologists, and the final diagnoses of focal liver lesions were reached by consensus involving histopathological data, findings at PET-CT and/or follow-up imaging studies. The study coordinators recorded the final diagnoses of all selected lesions and their location according to Couinaud's segmental anatomy (the middle hepatic vein was used as an anatomical reference to divide the liver into left hepatic lobe and right hepatic lobe). The size of lesions in the 58 patients with focal liver lesions of the same etiology in left and right hepatic lobes was determined by the largest diameter as displayed on

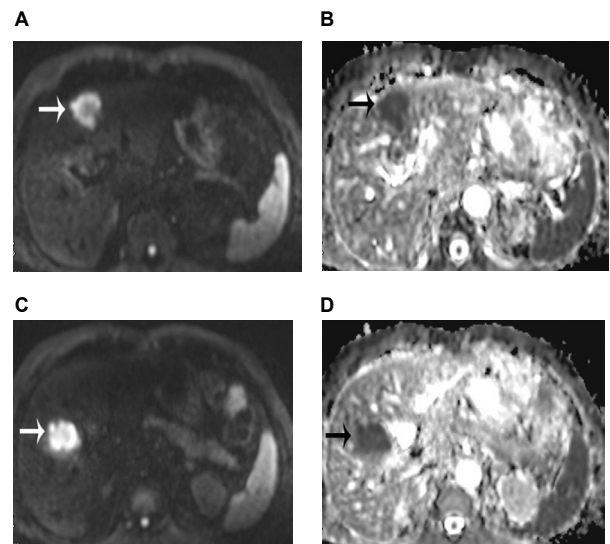


Figure 2. Two Metastases of Colon Cancer from A 63-year-old Male. (A and C) Metastases in both lobes showing restricted diffusion with high signal on diffusion-weighted imaging ($b = 800 \text{ sec/mm}^2$). (B and D) ADC map.

combined images of DW imaging, T2 weighted imaging and dynamic contrast-enhanced imaging.

The region of interest (ROI) was placed on ADC maps by a single radiologist (X.H., with 6 years of experience in the interpretation of body magnetic resonance images) to avoid inter-observer bias. ROIs of focal liver lesions were placed within the solid part of lesions as large as possible, avoiding necrosis and cystic degeneration, which showed no enhancement on dynamic contrast-enhanced magnetic resonance images. ROIs of normal liver parenchyma were drawn as large as possible without involving intrahepatic vessels and this procedure was performed carefully to exclude motion artifacts. The mean ADCs were calculated by averaging ADCs of all ROIs in each lesion.

Statistical analysis

In the 58 patients with focal liver lesions of the same etiology in left and right hepatic lobes, sizes of focal liver lesions in left hepatic lobe and right hepatic lobe were compared using paired t-test. ADCs of normal liver parenchyma and benign and malignant focal liver lesions between the left hepatic lobe and right hepatic lobe were compared using paired t-test. In all 269 patients, the mean ADCs of CCC, HCC and metastases were compared using Analysis of Variance. The mean ADCs of hemangioma and focal nodular hyperplasias were compared using independent-sample t-test. The mean ADCs between benign and malignant focal liver lesions were compared using independent-sample t-test in left hepatic lobe and in right hepatic lobe. Receiver operating characteristic (ROC) curve analysis was used to test the ability of ADCs in differentiating malignant from benign focal liver lesions in left hepatic lobe, right hepatic lobe and whole liver. The areas under the ROC curve (AUC) was calculated and compared between left hepatic lobe and whole liver, as well as right hepatic lobe and whole liver. The optimal ADC cutoffs in left hepatic lobe, right hepatic lobe and whole liver were determined by ROC analysis and Youden index and $p < 0.05$ was considered to have

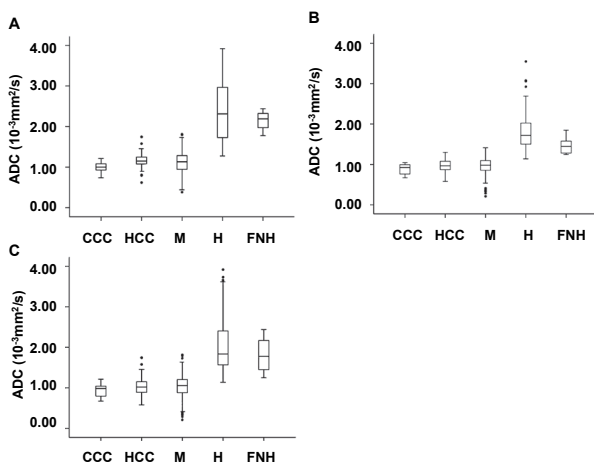


Figure 3. Box Plots of ADCs for Each Type of Focal Liver Lesion in (A) Left Hepatic Liver, (B) Right Hepatic Liver, and (C) Whole Liver. Median is shown as a line crossing each bar; dark spot denotes outliers. CCC, cholangiocellular carcinomas; HCC, hepatocellular carcinomas; M, metastasis; H, hemangioma; FNH, focal nodular hyperplasia.

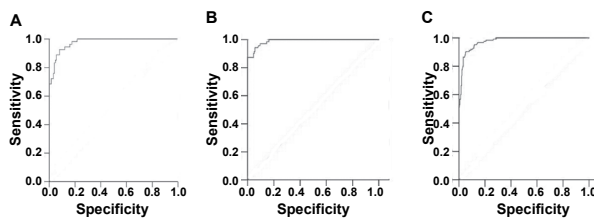


Figure 4. Receiver Operating Characteristic Curve Showing Comparison of Diagnostic Accuracy in Differentiating Malignant Focal Liver Lesions from Benign Focal Liver Lesions in (A) Left Hepatic Lobe, (B) Right Hepatic Lobe, and (C) Whole Liver. The area under the curve is 0.977, 0.990, and 0.976, respectively.

statistically significant difference. All statistical analyses were performed using SPSS version 17.0 for Windows.

Results

ADC measurements by dividing liver into left hepatic lobe and right hepatic lobe resulted in significantly different values

To compare the ADCs between the left and right hepatic lobes, we selected the focal liver lesions with similar average sizes in left hepatic lobe and right hepatic lobe (3.15±1.72cm vs 3.35±1.77cm; P = 0.236). The normal liver parenchyma and benign and malignant focal liver lesions in left hepatic lobe showed increased signal on ADC map compared with those in the right hepatic lobe, indicating higher ADC values in left hepatic lobe compared with right hepatic lobe, which was confirmed by quantitative ADC measurements: 1.58×10⁻³mm²/sec vs 1.36×10⁻³mm²/sec (Figure 1, Figure 2, Table 2). This observation suggested that ADC measurements by dividing liver into left hepatic lobe and right hepatic lobe resulted in significantly different values

Malignant lesions and benign lesions can be distinguished in left hepatic lobe, right hepatic lobe and whole liver by analyzing the ADCs using ROC curves

To evaluate the focal liver lesions in all the patients,

Table 3. ADCs of Focal Liver Lesions (means±standard Deviation; ×10⁻³ mm²/sec) in All Patients

| | LHL | RHL | WL |
|-------------------|-----------|-----------|-----------|
| Malignant lesions | 1.12±0.27 | 0.96±0.21 | 1.02±0.25 |
| CCC | 0.99±0.15 | 0.89±0.14 | 0.95±0.15 |
| HCC | 1.17±0.24 | 0.97±0.16 | 1.03±0.20 |
| Metastases | 1.12±0.29 | 0.95±0.26 | 1.03±0.29 |
| Benign lesions | 2.34±0.72 | 1.82±0.51 | 2.05±0.66 |
| Hemangiomas | 2.36±0.74 | 1.85±0.51 | 2.07±0.67 |
| FNH | 2.15±0.28 | 1.48±0.25 | 1.78±0.43 |

*Note: LHL, left hepatic lobe; RHL, right hepatic lobe; WL, whole liver; CCC, cholangiocellular carcinoma; HCC, hepatocellular carcinoma; FNH, focal nodular hyperplasia.

Table 4. Accuracy of Variable ADC Cutoffs for Distinguishing Malignant from Benign FLLs in LHL, RHL and WL

| | Cutoff [×10 ⁻³ mm ² /sec] | Sensitivity (%) | Specificity (%) | Accuracy (%) | Youden index |
|-----|--|--------------------|--------------------|-----------------|-----------------|
| LHL | 1.46 | 92.6 | 92 | 97.7 | 0.846 |
| RHL | 1.25 | 94.4 | 94.4 | 99 | 0.888 |
| WL | 1.41 | 90.4 | 94.7 | 97.6 | 0.851 |

*Note: FLL, focal liver lesions; LHL, left hepatic lobe; RHL, right hepatic lobe; WL, whole liver.

we calculated the mean ADCs of each type of focal liver lesions, plotted the box plots of ADCs and analyzed the data using ROC curves. Our data showed that 179 of the 429 focal liver lesions (42%) were located in left hepatic lobe and the remaining 250 focal liver lesions (58%) were located in right hepatic lobe. ADCs of metastases overlapped strongly with those of HCC and CCC in left hepatic lobe, right hepatic lobe and whole liver, without statistically significant difference (p>0.05) (Table 3, Figure 3). ADCs of hemangiomas overlapped with that of focal nodular hyperplasias, without statistically significant difference in left hepatic lobe and whole liver, but with statistically significant difference in right hepatic lobe (Table 3, Figure 3).

The mean ADC of benign focal liver lesions was significantly higher (p< 0.001 for all) than that of malignant ones in left hepatic lobe (2.34±0.72×10⁻³mm²/sec vs 1.12±0.27×10⁻³mm²/sec), right hepatic lobe (1.82±0.51×10⁻³mm²/sec vs 0.96±0.21×10⁻³mm²/sec) and whole liver (2.05±0.66×10⁻³mm²/sec vs 1.02±0.25×10⁻³mm²/sec) (Table 3). ROC curve analysis showed that ADCs obtained with b values of 0 and 800 sec/mm² were highly predictive for distinguishing malignant from benign focal liver lesions in left hepatic lobe, right hepatic lobe and whole liver, with the AUC being 0.977, 0.990 and 0.976 (Figure 4). For distinguishing malignant lesions from benign lesions, the sensitivity and specificity were 90.4% and 94.7% when cutoff (mm²/sec) was 1.41×10⁻³ in whole liver, 92.6% and 92.0% when cutoff was 1.46×10⁻³ in left hepatic lobe, and 94.4% and 94.4% when cutoff was 1.25×10⁻³ in right hepatic lobe (Table 4). The AUC of right hepatic lobe was higher than the AUC of whole liver (p< 0.05), but there was no significant difference between the AUC for left hepatic lobe and whole liver (p> 0.5). The accuracy of optimal ADC cutoffs for distinguishing malignant lesions from benign lesions in left hepatic lobe, right hepatic lobe and whole liver was shown in

Table 4. These data indicated that malignant lesions and benign lesions can be distinguished in left hepatic lobe, right hepatic lobe and whole liver by analyzing the ADCs using ROC curves.

Discussion

For focal liver lesions that have no significant difference in sizes between left hepatic lobe and right hepatic lobe, our results showed that, even when obtained in the same patient during the same MRI examination, ADCs of normal liver parenchyma, as well as benign and malignant focal liver lesions, were significantly higher in left hepatic lobe than in right hepatic lobe. The reason for selecting focal liver lesions with similar sizes is to exclude ADC difference caused by the sizes of focal liver lesions (Bruegel et al., 2008). In addition, our results were consistent with previous concepts and studies (Mürtz et al., 2002; Nasu et al., 2006; Kiliçkesmez et al., 2008; Kandpal et al., 2009; Kwee et al., 2009; Taouli and Koh DM, 2010; Schmid-Tannwald et al., 2013). The results suggested this bias may affect the performance of DWI in differentiating malignant focal liver lesions from benign focal liver lesions when selecting ADC cutoffs.

This source of bias may be mainly caused by cardiac motion (Mürtz et al., 2002; Nasu et al., 2006; Kandpal et al., 2009; Kwee et al., 2009; Dietrich et al., 2010; Taouli and Koh DM, 2010). In left hepatic lobe which is close to heart, cardiac motion results in spin dephasing that causes artifacts. Such artifacts are worse at higher b values and can result in spuriously high ADCs over the left hepatic lobe (Mürtz et al., 2002; Nasu et al., 2006). Furthermore, cardiac motion may accelerate the Brownian movement that leads to high ADCs over the left hepatic lobe. One way to minimize such artifacts is to use pulse (Mürtz et al., 2002) or cardiac triggering (Koh et al., 2007) at image acquisition. However, the use of pulse or electrocardiogram-triggered acquisitions that prolong the examination time can be difficult to implement (Taouli and Koh, 2010). Therefore, DWI of the liver in clinical practice is routinely obtained without cardiac gating.

In all patients, our study showed that ADCs were highly predictive for distinguishing malignant focal liver lesions from benign focal liver lesions in left hepatic lobe, right hepatic lobe and whole liver, with the AUC being 0.977, 0.990 and 0.976, respectively. In addition, the AUC of right hepatic lobe was higher than the AUC of whole liver ($p < 0.05$), suggesting that optimal ADC cutoff of right hepatic lobe can improve the diagnostic accuracy for focal liver lesions in right hepatic lobe when the liver was divided into left hepatic lobe and right hepatic lobe instead of being regarded as a whole. The result may be useful for focal liver lesions located in right hepatic lobe, but this difference was not found between left hepatic lobe and the whole liver ($p > 0.5$). The possible explanation is that inaccuracies of the ADCs of focal liver lesions located in left hepatic lobe caused by cardiac motion resulted in a relative lower diagnostic accuracy in left hepatic lobe than in right hepatic lobe. This may also be the reason for a relative lower diagnostic accuracy in whole liver than in right hepatic lobe.

Here, we describe the ADC cutoffs in left hepatic lobe, right hepatic lobe and whole liver, respectively. The ADC cutoffs of left hepatic lobe and whole liver were partially similar to those in previous studies (Taouli et al., 2003; Gourtsoyianni et al., 2008). Investigators in a recent meta-analysis (Xia et al., 2010) reported an AUC of the summary ROC of 0.96, with the sensitivity ranging from 0.74-1.0 (mean, 0.91) and the specificity ranging from 0.77-1.00 (mean, 0.93), when different ADC cutoffs ($1.4-1.6 \times 10^{-3} \text{mm}^2/\text{sec}$) were described. In general, the variation in ADC cutoffs can be partially attributed to the differences in multiple factors, such as differences in DWI technique applied for image acquisition, field strength, the choice of b values and the assessed liver lesions (Taouli and Koh, 2010; Zhang et al., 2010; Taouli, 2012). The b values were an important source of variability in ADC measurement for image acquisition. Zhang et al. (Zhang et al., 2010) pointed out that ADCs measured with low b values showed high variations. Therefore, higher b values result in more accurate ADCs (Dong and Liu, 2012). However, due to the relatively short T2 relaxation time of the normal liver parenchyma (approximately 24 ms at 3.0 T) (de Bazelaire et al., 2004), the b values used for clinical imaging are typically no higher than 1,000 sec/mm^2 (Taouli and Koh, 2010). A previous study showed that respiration-triggered DW-SS-EPI had better overall liver image quality and a significantly higher lesion-to-liver contrast ratio compared with those of breath-hold DW-SS-EPI (Sandberg et al., 2006). In this study, we chose respiration-triggered DW-SS-EPI sequence and relatively high b values (0 and 800 sec/mm^2). The composition and proportion of focal liver lesions were difficult to control because of lesion incidence. For our study, exclusion of simple cysts and lack of focal nodular hyperplasia and adenoma may be the factors leading to the variation in ADC cutoffs.

Furthermore, ADC cutoff of right hepatic lobe in our study was smaller compared to that of whole liver in previous studies (Ichikawa et al., 1998; Kim et al., 1999; Taouli et al., 2003; Bruegel et al., 2008; Erturk et al., 2008; Gourtsoyianni et al., 2008; Parikh et al., 2008; Vossen et al., 2008). In addition to the above reasons, the variability can be partially attributed to the difference of research objects. The liver was regarded as a whole in previous studies, but divided into left hepatic lobe and right hepatic lobe in our study. For the right hepatic lobe, this may reduce the impact due to relatively lower diagnostic accuracy in left hepatic lobe. Our study also showed that, in order to differentiate malignant focal liver lesions from benign focal liver lesions in right hepatic lobe, relatively high sensitivity (94.4%), specificity (94.4%) and accuracy (99%) can be achieved with an ADC cutoff of $1.25 \times 10^{-3} \text{mm}^2/\text{sec}$.

Therefore, although the ADCs of focal liver lesions in left hepatic lobe are sensitive to motion, DWI still appears to be a powerful tool for the differentiation of benign and malignant focal liver lesions, especially for focal liver lesions in right hepatic lobe.

However, the present study has some limitations. First, it was a single-center study, and only b values of 0 and 800 sec/mm^2 were used in obtaining DWI. Second, the number of focal nodular hyperplasia cases was small, but with

statistically significant differences. In addition, hepatic adenoma was absent in this study for its rare incidence. Finally, our retrospective study design did not allow us to assess the effect of cardiac motion, as all DWI scans were performed only with respiration-triggered DWI.

In our limited study, ADCs of normal liver parenchyma and benign and malignant focal liver lesions in left hepatic lobe calculated from noncardiac-gated DWI acquisitions were significantly higher compared with those in right hepatic lobe. ADCs were highly predictive for distinguishing malignant focal liver lesions from benign focal liver lesions in left hepatic lobe, right hepatic lobe and whole liver. When dividing the liver into left hepatic lobe and right hepatic lobe instead of regarding the liver as a whole, optimal ADC cutoff for focal liver lesions in right hepatic lobe can achieve higher diagnostic accuracy compared with that in whole liver, but this was not the case in left hepatic lobe. This finding may help improve the diagnosis of the focal liver lesions in right hepatic lobe.

Acknowledgements

This study was supported by Shandong Province Science and Technology Development Plan (No. 2012GSF11820), Shandong Province Science and Technology Development Plan (No. 2012YD18053) and Shandong Province Outstanding Young Scientist Award Fund (No. 2010BSB14072).

References

- Bartolozzi C, Cioni D, Donati F, et al (2001). Focal liver lesions: MR imaging-pathologic correlation. *Eur Radiol*, **11**, 1374-88.
- Bruegel M, Holzapfel K, Gaa J, et al (2008). Characterization of focal liver lesions by ADC measurements using a respiratory triggered diffusion-weighted single-shot echo-planar MR imaging technique. *Eur Radiol*, **18**, 477-85.
- de Bazelaire CM, Duhamel GD, Rofsky NM, et al (2004). MR imaging relaxation times of abdominal and pelvic tissues measured *in vivo* at 3.0 T: preliminary results. *Radiology*, **230**, 652-9.
- Dietrich O, Biffar A, Baur-Melnyk A, et al (2010). Technical aspects of MR diffusion imaging of the body. *Eur Radiol*, **76**, 314-22.
- Dong Y, Liu Q (2012). Differentiation of Malignant From Benign Pheochromocytomas With Diffusion-Weighted and Dynamic Contrast-Enhanced Magnetic Resonance at 3.0 T. *J Comput Assist Tomogr*, **36**, 361-6.
- Erturk SM, Ichikawa T, Sano K, et al (2008). Diffusion-weighted magnetic resonance imaging for characterization of focal liver masses: impact of parallel imaging (SENSE) and b value. *J Comput Assist Tomogr*, **32**, 865-71.
- Gourtsoyianni S, Papanikolaou N, Yarmenitis S, et al (2008). Respiratory gated diffusion-weighted imaging of the liver: value of apparent diffusion coefficient measurements in the differentiation between most commonly encountered benign and malignant focal liver lesions. *Eur Radiol*, **18**, 486-92.
- Griswold MA, Jakob PM, Heidemann RM, et al (2002). Generalized autocalibrating partially parallel acquisitions (GRAPPA). *Magn Reson Med*, **47**, 1202-10.
- Horton KM, Bluemke DA, Hruban RH, et al (1999). CT and MR imaging of benign hepatic and biliary tumors. *Radiographics*, **19**, 431-51.
- Ichikawa T, Haradome H, Hachiya J, et al (1998). Diffusion-weighted MR imaging with a single-shot echoplanar sequence: detection and characterization of focal hepatic lesions. *AJR Am J Roentgenol*, **170**, 397-402.
- Kandpal H, Sharma R, Madhusudhan KS, Kapoor KS (2009). Respiratory-triggered versus breath-hold diffusion-weighted MRI of liver lesions: comparison of image quality and apparent diffusion coefficient values. *AJR Am J Roentgenol*, **192**, 915-22.
- Kiliçkesmez O, Yirik G, Bayramoğlu S, et al (2008). Non-breath-hold high b-value diffusion-weighted MRI with parallel imaging technique: apparent diffusion coefficient determination in normal abdominal organs. *Diagn Interv Radiol*, **14**, 83-7.
- Kim T, Murakami T, Takahashi S, et al (1999). Diffusion-weighted single-shot echo planar MR imaging for liver disease. *AJR Am J Roentgenol*, **173**, 393-8.
- Koh DM, Takahara T, Imai Y, et al (2007). Practical aspects of assessing tumors using clinical diffusion-weighted imaging in the body. *Magn Reson Med Sci*, **6**, 211-24.
- Kwee TC, Takahara T, Niwa T, et al (2009). Influence of cardiac motion on diffusion-weighted magnetic resonance imaging of the liver. *MAGMA*, **22**, 319-25.
- Mürtz P, Flacke S, Träber F, et al (2002). Abdomen: diffusion-weighted MR Imaging with pulse-triggered single-shot sequences. *Radiology*, **224**, 258-64.
- Naganawa S, Kawai H, Fukatsu H, et al (2005). Diffusion-weighted imaging of the liver: technical challenges and prospects for the future. *Magn Reson Med Sci*, **31**, 175-86.
- Nasu K, Ku roki Y, Sekiguchi R, et al (2006). Measurement of the apparent diffusion coefficient in the liver: is it a reliable index for hepatic disease diagnosis?. *Radiat Med*, **24**, 438-44.
- Nasu K, Kuroki Y, Nawano S, et al (2006). Hepatic metastases: diffusion-weighted sensitivity-encoding versus SPIO-enhanced MR Imaging. *Radiology*, **239**, 122-30.
- Naiki T, Okamura T, Nagata D, et al (2011). Preoperative prediction of neurovascular bundle involvement of localized prostate cancer by combined T2 and diffusion-weighted imaging of magnetic resonance imaging, number of positive biopsy cores, and Gleason score. *Asian Pac J Cancer Prev*, **12**, 909-13.
- Parikh T, Drew SJ, Lee VS, et al (2008). Focal liver lesion detection and characterization with diffusion-weighted MR imaging: comparison with standard breath-hold T2-weighted imaging. *Radiology*, **246**, 812-22.
- Sandberg A, Parikh T, Johnson G, et al (2006). Feasibility of a respiratory-triggered SSEPI diffusion-weighted sequence for liver imaging using navigator echo technique: comparison with breath-hold diffusion-weighted sequence. *Proc Intl Soc Mag Reson Med*, **14**, 400.
- Schmid-Tannwald C, Jiang Y, Dahi F, et al (2013). Diffusion-Weighted MR Imaging of Focal Liver Lesions in the Left and Right Lobes: Is There a Difference in ADC Values?. *Acad Radiol*, **20**, 440-5.
- Taouli B (2012). Diffusion-weighted MR imaging for liver lesion characterization: a critical look. *Radiology*, **262**, 378-80.
- Taouli B, Koh DM (2010). Diffusion-weighted MR imaging of the liver. *Radiology*, **254**, 47-66.
- Taouli B, Vilgrain V, Dumont E, et al (2003). Evaluation of liver diffusion isotropy and characterization of focal hepatic lesions with two single-shot echo-planar MR imaging sequences: prospective study in 66 patients. *Radiology*, **226**, 71-8.
- Vossen JA, Buijs M, Liapi E, et al (2008). Receiver operating characteristic analysis of diffusion-weighted magnetic resonance imaging in differentiating hepatic hemangioma from other hypervascular liver lesions. *J Comput Assist Tomogr*, **32**, 750-6.
- Wu QW, Yan RF, Li Q, et al (2013). Magnetic resonance image manifestations of the atypical meningioma. *Asian Pac J Cancer Prev*, **14**, 6337-40.
- Xia D, Jing J, Shen H, et al (2010). Value of diffusion-weighted magnetic resonance images for discrimination of focal benign and malignant hepatic lesions: a meta-analysis. *J Magn Reson Imaging*, **32**, 130-7.
- Zhang JL, Sigmund EE, Chandarana H, et al (2010). Variability of renal apparent diffusion coefficients: limitations of the monoexponential model for diffusion quantification. *Radiology*, **254**, 783-92.